
This is an electronic reprint of the original article.
This reprint *may differ from the original in pagination and typographic detail.*

Author(s): Pakkanen, Kirsi; Karttunen, Jenni; Virtanen, Salla; Vuento, Matti

Title: Sphingomyelin induces structural alteration in canine parvovirus capsid

Year: 2008

Version:

Please cite the original version:

Pakkanen, K., Karttunen, J., Virtanen, S., & Vuento, M. (2008). Sphingomyelin induces structural alteration in canine parvovirus capsid. *Virus Research*, 132, 187-191.
<https://doi.org/10.1016/j.virusres.2007.10.008>

All material supplied via JYX is protected by copyright and other intellectual property rights, and duplication or sale of all or part of any of the repository collections is not permitted, except that material may be duplicated by you for your research use or educational purposes in electronic or print form. You must obtain permission for any other use. Electronic or print copies may not be offered, whether for sale or otherwise to anyone who is not an authorised user.

Sphingomyelin induces structural alteration in canine parvovirus capsid

Kirsi Pakkanen, Jenni Karttunen, Salla Virtanen, Matti Vuento

Virus Research 132 (2008) 187–191

Nanoscience Center, Department of Biological and Environmental Science, University of Jyväskylä, Finland

Keywords: Canine parvovirus; Sphingomyelin; Acidic pH; Tryptophan fluorescence; Circular dichroism

Abstract

One of the essential steps in canine parvovirus (CPV) infection, the release from endosomal vesicles, is dominated by interactions between the virus capsid and the endosomal membranes. In this study, the effect of sphingomyelin and phosphatidyl serine on canine parvovirus capsid and on the phospholipase A2 (PLA2) activity of CPV VP1 unique N-terminus was analyzed. Accordingly, a significant ($P \leq 0.05$) shift of tryptophan fluorescence emission peak was detected at pH 5.5 in the presence of sphingomyelin, whereas at pH 7.4 a similar but minor shift was observed. This effect may relate to the exposure of VP1 N-terminus in acidic pH as well as to interactions between sphingomyelin and CPV. When the phenomenon was further characterized using circular dichroism spectroscopy, differences in CPV capsid CD spectra with and without sphingomyelin and phosphatidyl serine were detected, corresponding to data obtained with tryptophan fluorescence. However, when the enzymatic activity of CPV PLA2 was tested in the presence of sphingomyelin, no significant effect in the function of the enzyme was detected. Thus, the structural changes observed with spectroscopic techniques appear not to manipulate the activity of CPV PLA2, and may therefore implicate alternative interactions between CPV capsid and sphingomyelin.

Canine parvovirus (CPV) is a member of the autonomous Parvovirus genus of Parvoviridae family (Tattersall and Cotmore, 1988) and has a diameter of approximately 26 nm (Agbandje et al., 1993 and Chapman and Rossmann, 1993), that is, of 260 Å. The capsid surface features 15 Å depressions at the twofold axes, 22 Å protrusions (spikes) at the threefold axes and channels surrounded by 15 Å depressions at fivefold axes (Tsao et al., 1991 and Wu and Rossmann, 1993). Like other parvoviruses, CPV has not been shown to contain lipids or carbohydrates (Berns, 1990).

The capsid is composed of 60 subunits, 90% of which are VP2 proteins (584 amino acid residues) and 10% VP1 proteins (727 amino acid residues), and arranged in icosahedral symmetry ($T = 1$). The third structural protein, VP3, is formed only in DNA containing capsids following cleavage of VP2 amino terminus by host cell proteases (Paradiso et al., 1982, Cotmore and Tattersall, 1987 and Reed et al., 1988). The monomers of the capsid are formed with eight-stranded antiparallel β -barrel, “jelly roll”, structure. The loops connecting barrel strands form partly the surface of the capsid (Tsao et al., 1991). One of the loops in CPV capsid is the site of an essential structural difference between CPV and its closest relative feline panleukopenia virus. The loop between residues 359 and 375 in these viruses differs in orientation and flexibility (Agbandje et al., 1995). The glycine residues at the ends of the loop have been shown to contribute to the flexibility. Also the three calcium-binding sites of the capsid affect the conformation of the loop in pH and Ca^{2+} concentration-dependent ways (Simpson et al., 2000).

The capsid protein VP1 contains the entire amino acid sequence of VP2 protein in addition to the unique N-terminus of 143 amino acid residues in length. While some of the VP2 N-termini are external, their glycine-rich sequence residing along the fivefold pore, all the VP1 N-termini are buried inside the capsid (Paradiso, 1981 and Weichert et al., 1998). The unique part of VP1 can be exposed *in vitro* using limited heating or urea (Weichert et al., 1998, Cotmore et al., 1999 and Vihinen-Ranta et al., 2002). In cells, the unique part of VP1 is known to change location relative to the capsid surface in the acidic environment of the late stages of endocytic route (Suikkanen et al., 2003 and Farr et al., 2006). In addition to this, Farr et al. have shown that acidity-triggered exposure of minute virus of mice VP1 N-terminus is sensitive to proteolytic cleavage of VP2 to form VP3 (Farr et al., 2006). Importantly, the exposure of VP1 N-termini has been shown to be critical for successful CPV infection (Suikkanen et al., 2003). The VP1 unique region of many parvoviruses, including CPV, has been shown to harbor two motifs. Firstly, the unique part of CPV contains basic sequences resembling classical nuclear localization signals (Vihinen-Ranta et al., 1997). Secondly, the unique part contains two motifs conserved in secretory phospholipase A₂ (sPLA₂): HDXXY (amino acid residues 46–51) found in catalytic sites and YXGXG (amino acid residues 20–25) known to be associated with Ca^{2+} -binding loops (Zádori et al., 2001). The unique terminus itself, as well as capsids exposed to acidic pH or heat, have been shown to exhibit phospholipase A₂ (PLA₂) activity (Suikkanen et al., 2003, Zádori et al., 2001 and Canaan et al., 2004). Certain properties of parvoviral PLA₂s differ from sPLA₂s. Parvoviral PLA₂s do not contain cysteine, the sequence connecting the two catalytic site helices is shorter and the YXGPG sequence of Ca^{2+} -binding loop is strictly conserved (Zádori et al., 2001). Parvoviral PLA₂s do not exhibit substantial specificity to substrates in terms of lipid species or the degree of saturation of sn – 2 acyl fatty acid chains, the latter being a typical feature of sPLA₂s (Zádori et al.,

2001 and Canaan et al., 2004). Another characteristic of sPLA₂s, Ca²⁺ dependence, is characteristic also for parvoviral PLA₂s. In addition, the PLA₂ region of VP1 unique part has been proposed to be able to bind one Ca²⁺ ion (Canaan et al., 2004). PLA₂ enzymes have higher activity towards membranes or aggregated lipids than lipids free in solution (Verger et al., 1973). This interfacial activation has also been shown with parvoviral phospholipases (Canaan et al., 2004).

Since the exposure of VP1 N-terminus is known to be closely associated with penetration of CPV through endosomal membranes (Weichert et al., 1998, Cotmore et al., 1999, Suikkanen et al., 2003 and Farr et al., 2006), it is fair to assume that important structural changes occur in the acidic conditions of the endosomal vesicles. However, the possible involvement of membranes during the exposure of the VP1 N-terminus or as a facilitator of other structural changes is currently unknown. Here, to gain insight into the effects of sphingomyelin and phosphatidyl serine bilayers combined with neutral and acidic pH on CPV capsids, tryptophan fluorescence and circular dichroism spectroscopy were utilized. In addition, the effect of sphingomyelin on CPV PLA₂ activity was characterized.

Canine parvovirus (CPV-2d) used in this study, originally derived from infectious plasmid clone of the virus (Parrish, 1991), was cultured and purified as previously described (Suikkanen et al., 2003) with the exception that the final pellet from ultracentrifugation was dissolved in a small volume of non-buffered saline and diluted with potassium phosphate for analysis. Pooled preparations of infectious CPV capsids containing DNA were used in all experiments except in CD spectroscopy, where pooled empty capsids (not containing DNA) were used to avoid contribution of DNA to CD signal. The purified virus stocks were characterized by polyacrylamide gel electrophoresis using 10% gels and coomassie brilliant blue staining. Concentration of virus was determined with Bradford assay using bovine serum albumin as a standard (Bio-Rad, Hercules, CA). Bovine brain phosphatidyl serine and bovine brain sphingomyelin were from Sigma Aldrich (St. Louis, MO). Lipids were dissolved in chloroform and dried with nitrogen-flow. To prepare small unilamellar vesicles (SUVs), lipids were resuspended in 10 mM potassium phosphate buffer (or in the case of sphingomyelin for PLA₂ activity studies: assay buffer) of desired pH to a final lipid concentration of 4 mg/ml. The suspension was vortexed for 20 min and sonicated with a tip sonifier (Branson, Danbury, CT) in an ice-water bath (Lee et al., 2001).

CPV capsid intrinsic tryptophan fluorescence was recorded at +25 °C using a Perkin Elmer LS55 fluorescence spectrophotometer and a cuvette with 10 mm path length (Perkin Elmer Industries, Wellesley, MA). Temperature was maintained within ±1 °C with Thermo Haake water bath and circulator (Thermo Electron Corporation, Waltham, MA). Samples were excited at 290 nm and non-corrected emission was measured at 310–430 nm. Final concentration of CPV in a cuvette was 2.5 µg/ml diluted in 10 mM potassium phosphate buffer at appropriate pH. Final concentration of CaCl₂ was 1 mM and of lipids (as SUVs) approximately 0.05 mg/ml. For the acidification studies CPV capsids were acidified with 0.1 M HCl (resulting as final pH of 5.5) for 10 min and subsequently neutralized with 0.1 M NaOH and diluted to measurement volume, resulting in final concentration of 2.5 µg/ml CPV. Excitation and emission slits were set at 2.5 nm. Background fluorescence of liposomes, CaCl₂ and buffer were subtracted from corresponding sample data. The

spectra were averaged from three scans and emission maxima taken from three sets of averaged results. The emission maxima data were analyzed using the unpaired Student's t-test with a two-tailed P-value, and statistical significance was determined relative to the control (CaCl₂ only) samples (**P < 0.05).

The CPV capsid contains approximately 850 tryptophan (Trp) residues (14 in each VP2 protein and 15 in each VP1 protein), mostly located inside the capsid subunits in positions most likely shielded from water molecules (Chapman and Rossmann, 1993, Reed et al., 1988 and Xie and Chapman, 1996). Tryptophan residues have emission maximum near 330 nm when located in hydrophobic environment and closer to 350 nm when in the hydrophilic areas of the protein. In some cases this red-shift is due to certain parts of the protein being moved closer to the surface of a protein complex as a result of conformational changes. On other occasions, the red-shift is influenced by access of aqueous buffer inside a protein or protein subunits of a larger multiprotein complex (Lacowicz, 1999 and Vivian and Callis, 2001), indicating loosening of binding interactions between subunits. Fluorescence of tryptophan residues, fully exposed to water, is not affected by changes in pH, as demonstrated with N-acetyl tryptophan amide (Luykx et al., 2004).

Here, environment-induced changes in CPV virions were monitored using the intrinsic fluorescence of Trp residues. CPV capsid is known to bind Ca²⁺ ions (Simpson et al., 2000), which may provide stabilization to the capsid structure. To mimic this effect of intracellular environment, fluorescence measurements with lipids were performed using CaCl₂-containing solutions. Red-shifts in emission peak position of Trp fluorescence of CPV were detected when the effect of sphingomyelin and phosphatidyl serine membranes were examined (Fig. 1A). At pH 5.5, sphingomyelin induced a statistically significant red-shift (3.8 ± 0.3 nm; P = 0.002) in tryptophan fluorescence. Similar, but statistically insignificant, red-shifts were observed also with sphingomyelin at pH 7.4 (5.9 ± 3.8 nm) and in the presence of phosphatidyl serine in both acidic and neutral conditions (4.2 ± 2.5 and 0.9 ± 1 nm, respectively). Phosphatidyl choline, phosphatidyl ethanolamine, and phosphatidyl inositol induced no apparent shifts in the emission peak positions (not shown). These results suggest that sphingomyelin- and possibly phosphatidyl serine-containing membranes induce structural changes to CPV capsid, leading to possible water penetration into the virion. To understand the effect of acidic conditions on CPV capsid more profoundly, CPV capsids were exposed shortly to pH 5.5 and neutralized after 10 min and analyzed with fluorescence spectroscopy (Fig. 1D). Despite the seeming decrease in emission peak wavelength, no statistically significant change in Trp fluorescence emission peak positions were detected (P = 0.458).

Results obtained with tryptophan fluorescence were further analyzed by circular dichroism spectroscopy in far UV region using a Jasco J-720 spectropolarimeter (JASCO Corporation, Tokyo, Japan) and a cylindrical quartz cuvette (Helma GmbH & Co KG, Müllheim, Germany) with a pathlength of 1 mm. Before use in CD measurements empty (not containing DNA) capsids of CPV were dialysed against 10 mM potassium phosphate buffer to avoid the effect of sodium ions on CD signal. 20 µg micrograms of capsids were used in each measurement. The spectra were recorded at 240–190 nm with bandwidth of 2.0 nm, 0.5 s response time. Scan speed was 10 nm/min. The spectra shown are

representative averages of three scans. Standard deviations shown in Fig. 1C are from five experiments. Final concentration of CaCl₂ was 1 mM in the cuvette. SUVs (prepared as described above) used in CD measurements were composed of phosphatidyl serine and sphingomyelin (molar ratio 1:1) with total lipid concentration of 4 mg/ml. Final concentration on lipids (as liposomes) in the cuvette was approximately 0.05 mg/ml. Baseline was measured with or without SUVs. The capsids for acidification studies were treated as described with tryptophan fluorescence measurements. 40 µg of capsids were used in each CD measurement. The spectra were drawn from data point values after subtraction of baseline, and fitted to Stineman function in the Kaleida Graph software Version 3.6.4 (Synergy Software, Reading, PA).

CD spectra of empty CPV capsids with Ca²⁺ and sphingomyelin-phosphatidyl serine liposomes or with Ca²⁺ only are presented in Fig. 1B and standard deviations of the 220–200 nm region of the spectra are in Fig. 1C. The overall form of the spectra features a wide negative valley at 220–200 nm and a positive peak at 190 nm. With Ca²⁺ only, the negative valley at 220–200 nm was less profound and the positive peak at 190 nm was lower at pH 5.5 than at pH 7.4. However, the presence of sphingomyelin-phosphatidyl serine liposomes with Ca²⁺ markedly changed the CD spectra of the capsids. At pH 7.4, the negative valley at 220–200 nm became less negative and the positive peak at 190 nm became more negative in the presence of liposomes and Ca²⁺ in comparison with Ca²⁺ only. On the contrary, at pH 5.5, the presence of liposomes shifted the 190 nm peak to a positive and the 220–200 nm valley to a more negative direction (and especially the 220 nm side of the valley). The CD data were not interpreted in terms of secondary structure. However, these data suggest that sphingomyelin-phosphatidyl serine membranes induce structural changes in CPV in both acidic and neutral conditions, supporting the results obtained with tryptophan fluorescence. The spectral change observed in acidic pH in the presence of Ca²⁺ without liposomes is likely to be at least partly associated with VP1 N-terminus exposure, but some other structural modifications need to be present to justify the differences between spectra with liposomes and with Ca²⁺ only. It is possible that these structural changes detected are, at least to some extent, responsible for the differences in water penetration into the capsid as detected with tryptophan fluorescence measurements. Also, the results of acidification/neutralization studies were further characterized with CD spectroscopy. The CD spectra (240–200 nm region) of native and acid-treated capsids are presented in Fig. 1E and standard deviations of the 220–200 nm region in Fig. 1F. The spectrum of acid-treated capsids resembles that of native capsids, but has some distinguishing features. The 220–200 nm valley is less profound in acid-treated capsids and there is a distinct shoulder at 225 nm. The differences in data obtained with acidified capsids with tryptophan fluorescence spectroscopy and CD spectroscopy are interesting and may relate to previously unknown long-term effects of the low pH step in CPV infection.

PLA₂ activities were measured using a commercial kit (Cayman Chemicals, Ann Arbor, MI, USA) with bee venom PLA2 as a control. For each sample, 35 µg CPV or bee venom PLA2 was used. In the case of added lipids, the reaction mixture was supplemented with 100 µg sphingomyelin as SUVs prepared (as above) in assay buffer. In reaction mixture without added sphingomyelin only assay buffer was used. Absorbances were measured using a Perkin Elmer Lambda 850 spectrophotometer. Temperature was maintained at

+25 °C using a water bath and circulator (Thermo Electron Corporation, Waltham, MA). PLA₂ activities were measured and calculated according to manufacturer's instructions. Enzyme activity in the presence of sphingomyelin was analyzed using the unpaired Student's t-test with a two-tailed P value, and statistical significance was determined relative to the control (no added lipid) samples (**P < 0.05).

To exclude the potential effect of these putative structural changes on PLA₂ function, the enzymatic activity of CPV PLA₂ was tested using thiol-phosphatidyl choline substrate supplemented with sphingomyelin. The results suggested CPV PLA₂ to function in the presence of sphingomyelin similarly as the bee venom PLA₂ used as a control. Since, the activity of CPV PLA₂ was only slightly decreased, from $0.0019 \pm 0.0003 \mu\text{mol (ml min)}^{-1}$ without sphingomyelin to $0.0016 \pm 0.00031 \mu\text{mol (ml min)}^{-1}$ with sphingomyelin (Fig. 2). This decrease was found to be statistically insignificant (P = 0.2621). It therefore seems that the addition of sphingomyelin into the reaction mixture has no significant effect on the activity of either CPV PLA₂. This further implies that the sphingomyelin-related conformational changes detected with spectroscopic methods most likely are not involved in facilitation of CPV PLA₂ function and may therefore suggest some other so far unknown mechanisms related to the endosomal escape process of CPV.

During its endocytic entry, CPV encounters the acidic intraendosomal environment. The virus travels to late endosomes and possibly even further to lysosomes. CPV is then released from these compartments to the cytoplasm, to undertake a further voyage to the nucleus (Suikkanen et al., 2003 and Reed et al., 1988). The exact mechanism of the release is unknown, although it has been shown that the CPV-containing endosomes are not broken down and become permeable only to particles smaller than approximately 10–20 kDa, as shown with dextran beads (Suikkanen et al., 2003) and with sarcin (Parker and Parrish, 2000). During the release, at the latest, CPV comes into contact with endosomal membranes. In addition, the virions appear to have affinity for some membrane lipids (Suikkanen et al., 2003). The low pH of endosomes is necessary for CPV release, as inhibitors of V-type ATPase, responsible for acidification of the endosomal lumen, retain CPV in the endosomes (Suikkanen et al., 2003 and Parker and Parrish, 2000). The release of CPV from late endosomal compartments is inhibited by PLA₂ inhibitors, strongly suggesting that the enzymatic activity has a crucial role during viral escape. However, exposure of the N-terminal domain and activation of PLA₂ assisted by endosomal conditions are probably not enough to promote the release, since endocytosed, pre-activated capsids are retained in the endosomes in the presence of V-ATPase inhibitors similarly to intact capsids (Suikkanen et al., 2003). Thus, other conformational rearrangements in the capsid that facilitate the endosomal escape may occur. Such changes could be related to low pH, but also to contact of capsids with endosomal membranes. In this study we have characterized lipid or membrane induced changes as well as acid-induced changes in CPV capsids. The data suggest that sphingomyelin induces changes in CPV capsids, which, at least to some extent, differ from those induced by acidic conditions. However, these changes do not seem to be related to PLA₂ activity of the capsid, which may indicate that membrane-capsid interactions have a role in the membrane penetration process of the virus even outside the scope of lipase action. In addition to this, we have shown that acidic conditions induce long-term changes in CPV

capsids. Even though the permeability to water seems to recover to almost original level after the capsid moves to neutral environment; some changes in the structure still remain. This may have significance in later steps of the viral life cycle.

Acknowledgements

We are especially grateful to Ms. Anna R. Mäkelä, MSc, for her valuable advice during the writing process. We also thank Dr. Tuula O. Jalonens for critically reading the manuscript, Pirjo Kauppinen for technical assistance and Dr. Ilkka Kilpeläinen and Dr. Tero Pihlajamaa for the use of CD spectroscopy facilities. This study was supported by a grant from the Rector of University of Jyväskylä and the National Graduate School in Nanoscience (K.P.) and by Academy of Finland (contract # 102161).

References

- M. Agbandje, R. McKenna, M.G. Rossmann, M.L. Strassheim, C.R. Parrish. Structure determination of feline panleukopenia virus empty particles. *Proteins*, 16 (2) (1993), pp. 155–171.
- M. Agbandje, C.R. Parrish, M.G. Rossmann. The structure of parvoviruses. *Semin. Virol.*, 6 (1995), pp. 299–309
- K.I. Berns, Parvovirus replication. *Microbiol. Rev.*, 54 (1990), pp. 316–329
- S. Canaan, Z. Zádori, F. Ghomashchi, J. Bollinger, M. Sadilek, M.E. Moreau, P. Tijssen, M.H. Gelb. Interfacial enzymology of parvovirus phospholipases A2. *J. Biol. Chem.*, 279 (15) (2004), pp. 14502–14508
- M.S. Chapman, M.G. Rossmann. Structure, sequence and function correlations among parvoviruses. *Virology*, 94 (1993), pp. 491–508
- S.F. Cotmore, P. Tattersall. The autonomously replicating parvoviruses of vertebrates. *Adv. Virus Res.*, 33 (1987), pp. 91–169
- S.F. Cotmore, A.M. D'abramo Jr., C.M. Ticknor, P. Tattersall. Controlled conformational transitions in the MVM virion expose the VP1 N-terminus and viral genome without particle disassembly. *Virology*, 254 (1999), pp. 169–181
- G.A. Farr, S.F. Cotmore, P. Tattersall. VP2 cleavage and the leucine ring at the base of the fivefold cylinder control pH-dependent externalization of both the VP1 N-terminus and the genome of minute virus of mice. *J. Virol.*, 80 (1) (2006), pp. 161–171
- J.R. Lacowicz. Principles of Fluorescence Spectroscopy. *Plenum Press*, NY, USA (1999)

S.-K. Lee, C. Dabney-Smith, D.L. Hacker, B.D. Bruce. Southern cowpea mosaic virus coat protein: the role of basic amino acids, helix-forming potential, and lipid composition. *Virology*, 291 (2001), pp. 299–310

D.M.A.M. Luykx, M.G. Casteleijn, W. Jiskoot, J. Westdijk, P.M.J.M. Jongen. Physicochemical studies on the stability of influenza haemagglutinin in vaccine bulk material. *Eur. J. Pharm. Sci.*, 23 (2004), pp. 67–75

P.R. Paradiso. Infectious processes of the parvovirus H-1: correlation of protein content, particle density, and viral infectivity. *J. Virol.*, 39 (3) (1981), pp. 800–807

P.R. Paradiso, S.L. III Rhode, I. Singer. Canine parvovirus: a biochemical and ultrastructural study. *J. Gen. Virol.*, 62 (1982), pp. 113–125

J.S. Parker, C.R. Parrish. Cellular uptake and infection by canine parvovirus involves rapid dynamin-regulated clathrin-mediated endocytosis, followed by slower intracellular trafficking. *J. Virol.*, 74 (4) (2000), pp. 1919–1930

C.R. Parrish. Mapping specific functions in the capsid structure of canine parvovirus and feline panleukopenia virus using infectious plasmid clones. *Virology*, 183 (1991), pp. 195–205

A.P. Reed, E.V. Jones, T.J. Miller. Nucleotide sequence and genome organization of canine parvovirus. *J. Virol.*, 62 (1) (1988), pp. 266–276

A.A. Simpson, V. Chandrasekar, B. Hebert, G.M. Sullivan, M.G. Rossmann, C.R. Parrish. Host range and variability of calcium binding by surface loops in the capsids of canine and feline parvoviruses. *J. Mol. Biol.*, 300 (2000), pp. 597–610

S. Suikkanen, M. Antila, A. Jaatinen, M. Vihinen-Ranta, M. Vuento. Release of canine parvovirus from endocytic vesicles. *Virology*, 316 (2) (2003), pp. 267–280

P. Tattersall, S.F. Cotmore. The nature of parvoviruses. *Parvoviruses and Human Disease* CRC Press, Boca Raton, FL (1988)

J. Tsao, M.S. Chapman, M. Agbandje, W. Keller, K. Smith, H. Wu, M. Luo, T.J. Smith, M.G. Rossmann, R.W. Compans, C.R. Parrish. The three-dimensional structure of canine parvovirus and its functional implications. *Science*, 251 (1991), pp. 1456–1464

R.M. Verger, C.E. Mieras, G.H. de Haas. Action of phospholipase A at interfaces. *J. Biol. Chem.*, 248 (1973), pp. 4023–4034

M. Vihinen-Ranta, L. Kakkola, A. Kalela, P. Vilja, M. Vuento. Characterization of a nuclear localization signal of canine parvovirus proteins. *Eur. J. Biochem.*, 1 (1997), pp. 389–394

M. Vihinen-Ranta, D. Wang, W.S. Weichert, C.R. Parrish. The VP1 N-terminal sequence of canine parvovirus affects nuclear transport of capsids and efficient cell infection. *J. Virol.*, 76 (4) (2002), pp. 1884–1891

J.T. Vivian, P.R. Callis. Mechanisms of tryptophan fluorescence shifts in proteins. *Biophys. J.*, 80 (2001), pp. 2093–2109

W.S. Weichert, J.S. Parker, A.T.M. Wahid, S.F. Chang, E. Meier, C.R. Parrish. Assaying for structural variation in the parvovirus capsid and its role in infection. *Virology*, 250 (1998), pp. 106–117

H. Wu, M.G. Rossmann. The canine parvovirus empty capsid structure. *J. Mol. Biol.*, 233 (1993), pp. 231–244

Q. Xie, M.S. Chapman. Canine parvovirus capsid structure, analyzed at 2.9 Å resolution. *J. Mol. Biol.*, 264 (1996), pp. 497–520

Z. Zádori, J. Szelei, M.-C. Lacoste, Y. Li, S. Gariepy, P. Raymond, M. Allaire, I.R. Nabi, P. Tijssen. A viral phospholipase A2 is required for parvovirus infectivity. *Dev. Cell*, 1 (2001), pp. 291–302

Figures

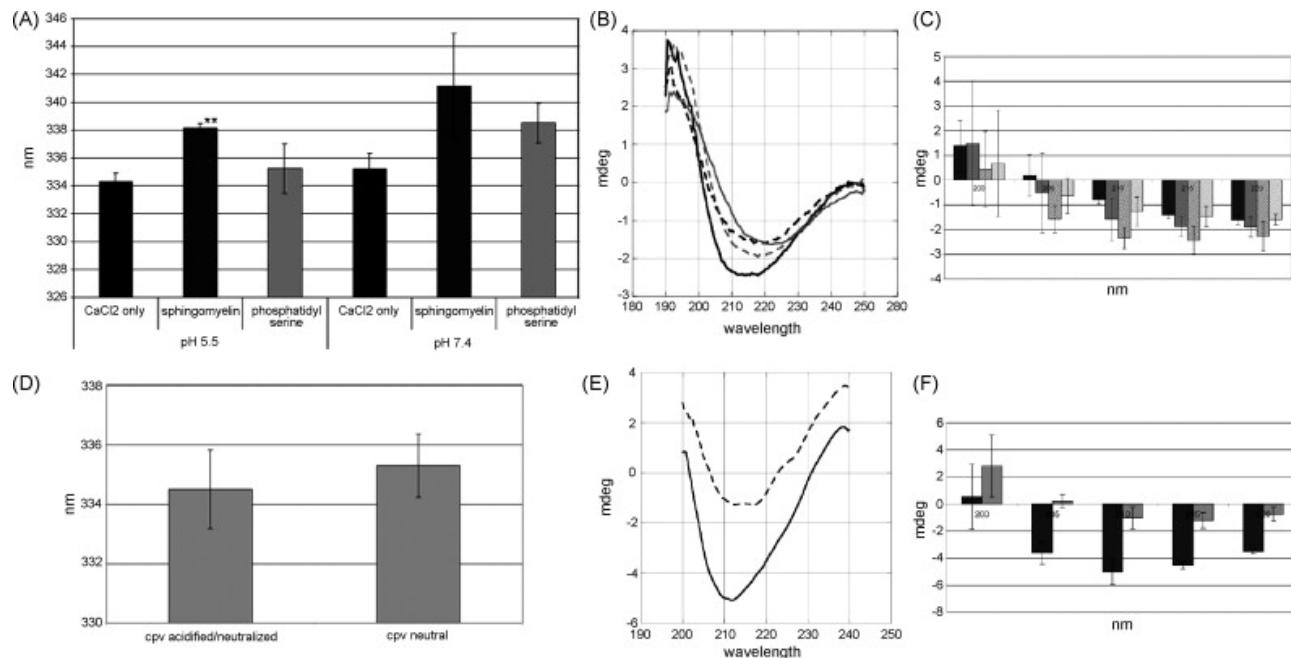


Figure 1 Intrinsic tryptophan fluorescence emission peak positions and CD spectra of CPV capsids with and without sphingomyelin and/or phosphatidyl serine. (A) Emission peak positions of CPV capsid intrinsic tryptophan fluorescence in 10 mM potassium phosphate buffer in +25 °C in the presence of 1mM CaCl₂ with and without sphingomyelin and phosphatidyl serine liposomes at pH 5.5 and 7.4. The data were compared using the unpaired Student's t-test with a two-tailed P value, and statistical significance was determined **P < 0.05. (B) CD spectra of empty CPV capsids in the presence of CaCl₂ with and without liposomes (sphingomyelin and phosphatidyl serine). CPV with CaCl₂ and liposomes at pH 5.5: (--) grey, CPV with CaCl₂ at pH 5.5: (—) grey, CPV with CaCl₂ and liposomes at pH 7.4: (--) black and CPV with CaCl₂ at pH 7.4: (—) black. (C) A blow up of the 220–200 nm region of the CD spectra in B with error bars indicating standard deviations. CPV with CaCl₂ at pH 5.5: dark grey, CPV with CaCl₂ and liposomes at pH 5.5: intermediate grey, CPV with CaCl₂ at pH 7.4: lighter grey and CPV with CaCl₂ and liposomes at pH 7.4: lightest grey. (D) Emission peak positions of CPV capsid intrinsic tryptophan fluorescence in neutral conditions with native capsids and capsids acidified at pH 5.5 for 10 min (and subsequently neutralized). (E) CD spectra of acidified and native CPV capsids in neutral conditions. Native CPV: (—) black and acidified CPV: (--) grey. (F) A blow up of 220–200 nm region of the CD spectra in (E) with error bars indicating standard deviations. Native CPV: dark grey and acidified CPV: light grey.

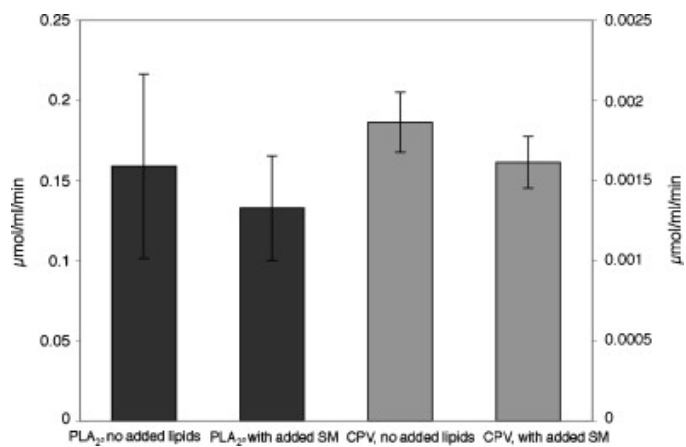


Figure 2 Activity of CPV PLA2 with and without sphingomyelin. Activities of CPV PLA2 and bee venom PLA2 with added and sphingomyelin and without added lipids. The vertical axis on the left corresponds to scaling of the values of PLA2 (dark grey) and the vertical axis on the right-hand side corresponds to scaling of the values of CPV (light grey).